A new in-beam proton therapy monitoring system based on digital MVT readout

Min Gao[1], Nicola D'Ascenzo[1], Hsien-Hsin Chen[3; 4], Fang-Hsin Chen[3], Ji-Hong Hong[4; 6], Ing-Tsung Hsiao[3],Tzu-Chen Yen[5], Jingfang Mao[7; 9], Jiade J. Lu[8; 9], Weidong Wang[10], Qingguo Xie[1; 2]

1Department of Biomedical Engineering, Huazhong Univ. of Sci. & Tech., Wuhan 2Wuhan National Laboratory for Optoelectronics, Wuhan 3Department of Medical Imaging and Radiological Science, Chang Gung University,Taoyuan 4Department of Radiation Oncology, Chang Gung Memorial Hospital at Linkou (CGMH at Linkou),Taoyuan 5Molecular Imaging Center and Nuclear Medicine, Chang Gung Memorial Hospital/Chang Gung University (CGMH/CGU), Taoyuan 6Institute for Radiological Research, Chang Gung Memorial Hospital/Chang Gung University(CGMH/CGU), Taoyuan 7Department of Thoracic Oncology, Shanghai Proton and Heavy Ion Center, Fudan University Cancer HospitalShanghai 8Department of Radiation Oncology, Shanghai Proton and Heavy Ion Center, Shanghai 9Shanghai Engineering Research Center of Proton and Heavy Ion Radiation TherapyShanghai 10Key Laboratory of Biomedical Engineering and Translational Medicine, Ministry of Industry and Information Technology, Beijing

Introduction

Positron Emission Tomography (PET) is one of the most accurate techniques used to retrieve the space distribution of the positron emitters produced by nuclear reaction within the target volume during and after proton irradiation and consequently to monitor the proton activity in biological targets. In-beam operation mode represents the modern frontier of proton therapy monitoring systems. PET detectors need to be integrated with the proton delivery equipment and the signal registration is performed either during irradiation or immediately after it without moving the patient. The in-beam signal registration is beneficial to increment the collected signal statistics and to reduce the effect of biological washout, with a consequent improvement of the image quality and accuracy. The key issue is here the high level of random coincidence background due to the prompt photons generated in nuclear interactions during proton irradiation. Modern solutions are based on two key-components. First the application of Silicon Photomultiplier (SiPM) sensors allows the miniaturization of the detection modules and the consequent improvement of the space and time resolution. Second the design of a fast digital readout electronics allows to increase the acquisition rate and enables an higher sensitivity during in-beam operation. As a possible solution to the high-rate challenge, we have previously proposed a digital multi voltage threshold (MVT) sampling method that takes samples of a pulse with respect to a set of four reference voltages. The total energy and the timing of the pulse can be obtained by the digital signal processing techniques. The combination of novel LYSO/SiPM sensor technology, MVT dedicated digital electronics and image reconstruction constitutes the Plug & Imaging (P&I) sensor.

Keywords: All-Digital PET, Proton Therapy Monitoring

Design and Implementation

The basic module of the P&I imaging sensor system is composed of a 6*6 LYSO array read out by a 6*6 SiPM array (FM30035; SENSL) and a printed circuit board (PCB) that provides the bias voltage to the SiPMs (Fig. 1a). The LYSO matrix contains 3.9*3.9*20*mm^3 pixellated crystals with 0.3 mm crystal gaps that are filled with barium sulfate to reflect the scintillation light and isolate each crystal optically.

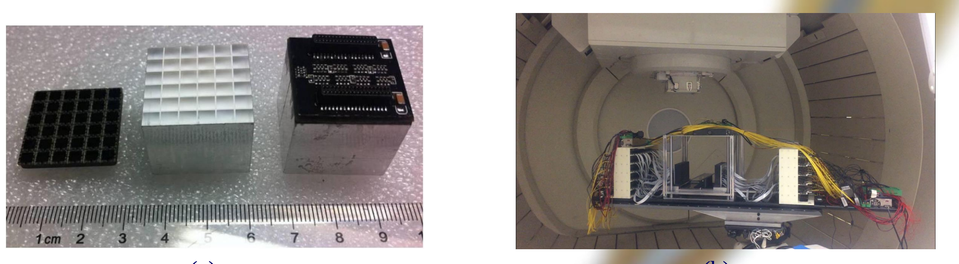

(a)

(b)

Fig. 1. Plug and imaging detection module (a) and installation of the 20*12.5 cm2 prototype inside the proton therapy treatment room at the proton therapy center of the Chang Gung Memorial Hospital (b). The prototype is shown during the table rotation to the final position.

We produced a prototype of proton therapy monitoring system (Fig. 1b) consisting of two flat panel PET heads, placed at a distance of 20 cm, and composed of a 8*5 P&I modules. The total area of each head is approximately 20*12.5 cm^2. A central support is used to align the target volume with the detector system and place it at the center of the field of view (FOV). An housing support for the 40 MVT boards is placed at both sides of the prototype and includes a fan cooling system. The whole structure is mounted on a proton therapy patient bed, which can be fixed to the movable stage.

The prototype was installed in the proton beam treatment room, aligned with the proton beam delivery system, at the proton therapy center of the Chang Gung Memorial Hospital of Taipei. We prepared a PMMA phantom and a water phantom with size 5*5*20 cm^2 and we irradiated them with a 150 MeV pencil beam aligned with its center. The beam had a Gaussian transversal profile with full width half maximum of approximately 2 mm and 0.3% energy spread. The irradiation was performed with an high proton statistics of approximately 1010 protons corresponding to a total dose of approximately 800 cGy delivered within a time of approximately 15 s. Data were acquired both during the beam-on time and during the following 3600 s after the beam is turned off (beam-off period). During the beam-on time we reached a saturated count rate of 5.2 Mcps. When the beam was off, the count rate decreased to 3.2 Mcps. After the phantom experiment, we performed preliminary animal irradiation in-beam monitoring. we irradiated a C57 mouse with a 70 MeV pencil beam for a total irradiation time of 250 s. Data were collected both during irradiation (beam-on) and for approximately 1000 s after irradiation (beam-off).

Results and Conclusions

The reconstructed measured lateral profile of the positron emitters produced in the water phantom during irradiation (beam on) is shown in Fig. 2a. The reconstructed measured lateral profile of the positron emitters produced in the PMMA phantom after irradiation (beam off) is shown in Fig. 2b. The width of the activity distribution in the y-direction perpendicular to the beam axis reflects the beam spot size, the scattering of the secondary particles produced in the target volume and the intrinsic experimental resolution of the detection system. The gray area corresponds to the reconstructed field of view. The estimated lengths of the activity profile are respectively (15.5 $\pm$ 0.50) cm and (13.33 $\pm$ 0.55) cm and are in agreement with the NIST tabulated values.

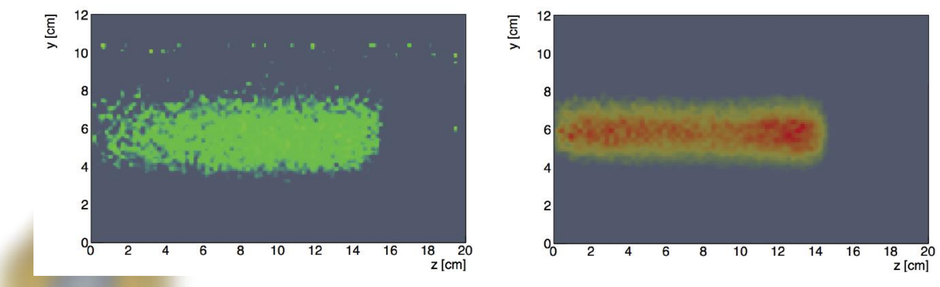

(a) (b)

Fig. 2. In-beam reconstruction of proton-induced positron activity in Water during beam-on irradiation (a) and in PMMA after irradiation (b).

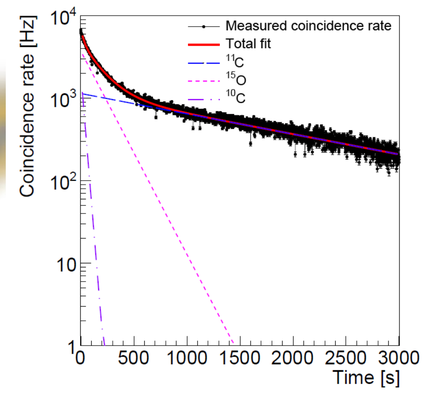

Fig. 3. Reconstruction of the time-dependent proton-induced positron activity in PMMA

The decay of the measured coincidence rate in the PMMA phantom after proton irradiation is shown in Fig. 3. The relative abundance of the produced ^{15}O,^{11}C and ^{10}C is estimated as 25.06%,72.85% and 2.58% with a relative accuracy of approximately 5%. Both fitted relative abundance and halflives were found in agreement with the physical expectation.

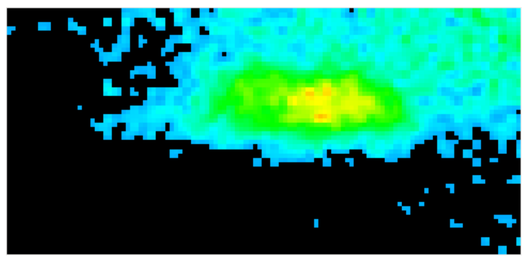

Fig. 4. In-beam reconstruction of proton-induced positron activity in C57 mouse

The reconstructed measured lateral profile of the positron emitters produced in the water phantom during irradiation (beam on) is shown in Fig. 4. and the irradiation direction is from right to left.

We demonstrated that the prototype is able to be operated during beam irradiation and provides a spatial reconstruction of the proton-induced positron emitters during both the irradiation (beam-on) high prompt photon background state and after the irradiation in the absence of prompt-photons, and proved the feasibility of all-digital PET in proton therapy monitoring.

Acknowledgment

This work was supported in part by the Natural Science Foundation of China (NSFC) (Grants 61425001, 61210003, and 61604059); in part by the Natural Science Foundation of Hubei Province (Grant 2016CFA005); in part by National Key Scientific Instrument and Equipment Development Program of China (2013YQ030923); in part by National Key Scientific Instrument and Equipment Development Program of Hubei Province (2013BEC050); in part by National Key Research and Development Program of China (2016YFF0101500); in part by 'the Fundamental Research Funds for the Central Universities' (2172018KFYXKJC049), (2017KFXKJC001).